PROCEEDINGS OF SPIE

Increasing baselines and precision of optical interferometers using two-photon interference

Michael Keach, Steve Bellavia, Zhi Chen, Jesse Crawford, Denis Dolzhenko, et al.

SPIE.

Increasing Baselines and Precision of Optical Interferometers Using Two-Photon Interference

Michael Keach[a], Steve Bellavia[a], Zhi Chen[a,c], Jesse Crawford[a], Denis Dolzhenko[a], Eden Figueroa[a,c], Aaron Mueninghoff[c], Andrei Nomerotski[a], Jonathan Schiff[a], Rom Simovitch[a], Anze Složar[a], Paul Stankus[a], and Stephen Vintskevich[b]

[a]Brookhaven National Laboratory, Upton NY 11973, USA
[b]Moscow Institute of Physics and Technology, Dolgoprudny, Moscow Region 141700, Russia
[c]Stony Brook University, Stony Brook, NY 11794, USA

ABSTRACT

Observations using interferometers provide sensitivity to features of images on angular scales much smaller than any single telescope, on the order of $\Delta\theta \sim \lambda/b$ where b is the interferometric baseline. Present-day optical interferometers are essentially classical, interfering single photons with themselves. However, there is a new wave of interest in interferometry using multiple photons, whose mechanisms are inherently quantum mechanical, which offer the prospects of increased baselines and finer resolutions among other advantages. We will discuss recent ideas and results for quantum-assisted interferometry using the resource of entangled pairs, and specifically a two-photon amplitude technique aimed at improved precision in astrometry.

Keywords: quantum astrometry, intensity interferometry, HBT effect, entangled photons

1. INTRODUCTION

Improving angular resolution in astronomical instrumentation has long been pursued in order to advance astrometric precision. Although traditional optical interferometry is a very successful astronomical technique, the required optical path between different detection stations to interfere photons limits baselines to hundreds of meters.[1, 2] This paper discusses the instrument requirements for a novel type of optical interferometer first proposed in our previous work[3, 4] that utilizes quantum mechanical interference effects between two photons from two astronomical sources. By using two sky sources, the proposed interferometer bypasses the traditional necessity of establishing a live optical path connecting detection sites, so the baseline distance can be made arbitrarily large, and consequently, an improvement of several orders of magnitude in angular resolution is in principle attainable. This development can be considered as a practical variation of pioneering ideas described in the work of Gottesman, Jennewein and Croke in 2012[5] to employ a source of single photons to measure the photon phase difference between the receiving stations, which were further developed in the following references.[6–9] At the same time, our ideas overlap with the Hanbury Brown & Twiss (HBT) intensity correlation astronomical technique,[10–12] which aims to resolve angular star dimensions employing two-photon enhancement effects.

There are many scientific opportunities that would benefit from substantial improvements in astrometric precision. Just to list a few: testing theories of gravity by direct imaging of black hole accretion discs, precision parallax and the cosmic distance ladder, mapping microlensing events, peculiar motions and dark matter; see[3] for a more comprehensive discussion. In this paper we briefly discuss the general setup of the interferometer in Section 2 and requirements for single photon detectors in Section 3. We then focus on the methods of analysis and recent experimental results in Section 4.

---

e-mails for correspondence: anomerotski@bnl.gov, mkeach@bnl.gov

2. TWO-PHOTON INTERFEROMETRY

The basic arrangement of the novel interferometer is shown in the left panel of Figure 1: the two sources 1 and 2 are both observed from each of two stations, **L** and **R**. Different optical schemes, using two or four telescopes, can be devised, but the key requirement is that photons from Source 1 be coupled into single spatial modes a at station **L** and e at station **R**; while those from Source 2 are separately coupled into the two single spatial modes b and f as shown.

The photon modes a and b at station **L** are then brought to the inputs of a symmetric beam splitter, with output modes labelled c and d; and the same for input modes e and f split onto output modes g and h at station **R**. The four outputs are then each viewed by a fast, single-photon sensitive detector. We imagine that the light in each output port is spectrographically divided into small bins and each spectral bin then constitutes a separate experiment with four detectors. If the two photons are close enough together in both time and frequency, then due to quantum mechanical interference the pattern of coincidences between measurements at "c" and "d" in **L** and "g" and "h" in **R** will be sensitive to the *difference* in phase differences $(\delta_1 - \delta_2)$; and this in turn will be sensitive to the relative opening angle between the two sources.
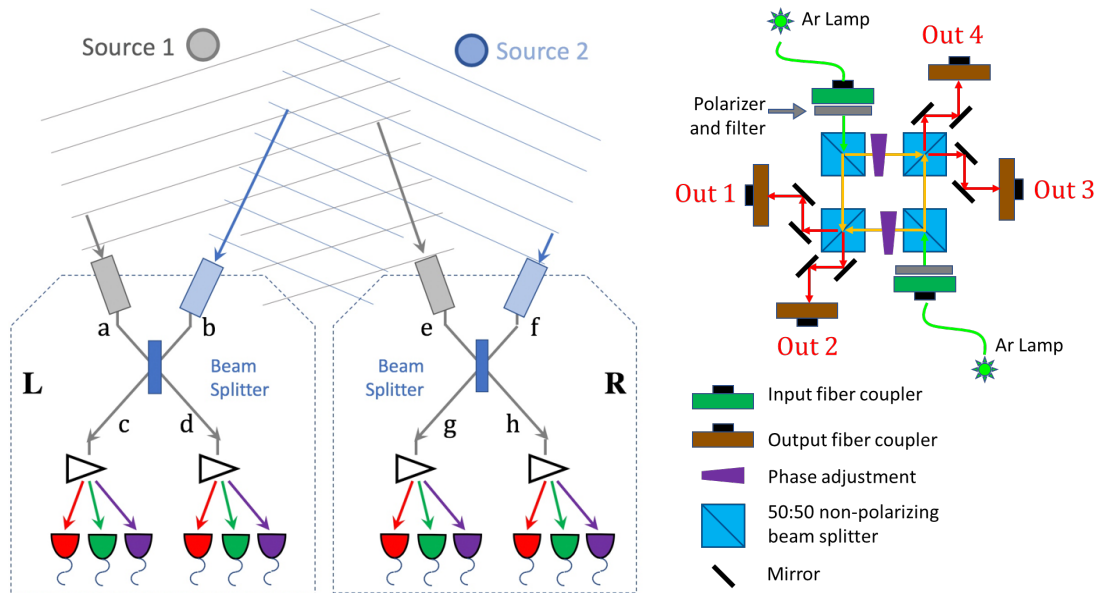

Figure 1. Left: Two-photon amplitude interferometer. Right: Block diagram of the bench analog, with components labeled.

In our previous work[3] we derived that the corresponding coincidence probabilities are equal to:

$$
\begin{aligned}
P(cg) &= P(dh) = (1/8)(1 + \cos(\delta_1 - \delta_2)) \\
P(ch) &= P(dg) = (1/8)(1 - \cos(\delta_1 - \delta_2)).
\end{aligned}
\tag{1}
$$

In this paper, we discuss a bench analog of the two astronomical source interferometer, which approximates astronomical sources using Argon lamps as a source of narrow-line thermal light. Using this bench analog, we utilize the Hanbury Brown & Twiss (HBT) intensity correlation astronomical technique,[10,11] to observe two-photon enhancement effects and then confirm oscillatory behavior in the rates of two-photon detections within a narrow time window surrounding the HBT peak. A block diagram of the bench analog as set up in lab is shown in the right part of Figure 1, along with the conceptual layout it is based on.

3. EXPERIMENTAL SETUP

3.1 Bench Analog

To approximate astronomical sources, two low pressure Argon lamps were used as quasi-thermal sources. A narrow-band filter (794.9 ± 1nm) was inserted between the Argon lamp and fiber coupler to isolate the 794.813nm spectral line. Photons originating from each argon lamp were coupled into single mode fibers leading to an adjustable fiber collimator which outputs the light to a 50:50 non-polarizing beamsplitter. Polarizers were also inserted after each input coupler and data was taken for three cases. First, no polarizers were inserted, for a baseline measurement. Next, polarizers were inserted in matching orientations; for example, both aligned vertically (V-V) which improved visibility. Finally polarizers were misaligned by 90 degrees, for example one aligned vertically, the other horizontally (V-H), which brings visibility to 0%.

The light from each lamp that is reflected in this beamsplitter then passes through a phase shifter, an asymmetric glass wedge mounted to a translation stage controlled by a stepper motor, before continuing to a second 50:50 non-polarizing beamsplitter, where it interferes with light from the opposite lamp that was transmitted through the first beamsplitter, which did not pass through a phase shifter. The interfered photons are coupled, both the reflected and transmitted portions, into single-mode fibers through collimating lenses, which were then read out by detectors, see 3.2.

The bench analog proved to be sensitive to vibration, so both passive and active isolation were used to counteract this. Additionally, all measurements were taken during periods of minimal noise as determined by stability measurements.

3.2 Photon Detection Instruments

Two fast timestamping technologies, single photon avalanche devices (SPAD) and superconducting nanowire single photon detectors (SNSPD), were considered as detection mechanisms.[4] SPAD sensors are based on silicon diodes with engineered junction breakdowns. They produce fast pulses with large enough amplitude to operate with single photon sensitiviy.[13–15] SPAD devices are capable of achieving timing resolution as good as 10 ps for single channel devices. These devices also have good scalability, with multichannel imagers already reported.[13,16]

SPADs were used for initial measurements, and on-sky testing is planned for the near future which may employ a SPAD array, but ultimately SNSPDs were chosen as the primary detection method for the below measurements. SNSPD is an emerging quantum technology which employs narrow, serpentine wires kept at a superconducting temperature by a helium compressor. When a photon deposits its energy in the vicinity of a wire, it momentarily breaks the superconductivity of the wire, inducing a voltage signal in the detection circuit.[17–19] We utilized a commercial multi-channel infrared-sensitive SNSPD system (SingleQuantum EOS) paired with a quTAG TDC model with a 7 ps timing resolution to record timestamps for each photon.

4. RESULTS AND ANALYSIS

4.1 Data Processing

The first step in the data processing was accounting for afterpulses, which likely appear because of non-ideal impedance matching in the front-end electronics. This lead to additional pulses delayed with respect to the primary signal by about 30 ns. Approximately 30% of pulses were followed by an afterpulse, see the delay distributions in the left part of Figure 2 for the precise fraction of afterpulses in each channel. To account for the afterpulses, all pulses registered within 35 ns of the previous hit in that channel were removed from the data.

The remaining data points are checked against data entries from other channel inputs for hits registered within ± 20 ns. Two-photon detections within this time window, or coincidences, are used for the calculations done in Section 4.2 and 4.3, where we discuss how these timestamps are used to determine where in time simultaneous pairs will appear and how to use this information to observe the phase shifting effects.
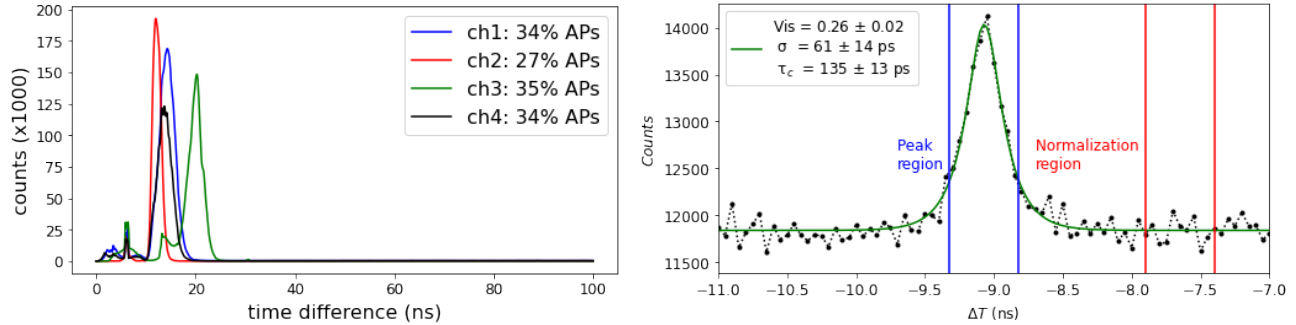
Figure 2. Left: Distribution of time difference between the main pulse and afterpulse for the four channels. Right: Example of the HBT peak fit with a Lorentzian function with decay time of 135 ps convoluted with experimental resolution of 61 ps.

4.2 Pair Correlations

As shown in Equation 1 and explicated in[3], due to the two-photon amplitude interference effect, the probability of a coincident detection between two channels at opposite detection sites (L and R) is sensitive to the phase difference between photons arriving at each detection site. Moreover, when a phase difference causes an enhancement in channel pairs (cg) and (dh), it simultaneously causes a reduction in the number of coincidences in channel pairs (ch) and (dg), and vice versa. Therefore, the number of coincidences (in the HBT peak region) in channel pairs (cg) and (dh) are expected to be correlated with each other and anticorrelated with those in channel pairs (ch) and (dg).

To test for these correlations between channel pairs, the number of coincidences within a $\pm 1.5\sigma$ window of the central peak in the coincidence distribution (determined via a Gaussian fit of the distribution) was recorded over the duration of experiment, typically around 30 minutes. This HBT peak region is represented by the blue vertical bars in the right plot of Figure 2.

Two-photon detections recovered from the processing algorithm are plotted in a histogram based on the time difference (Δt) between them, in nanoseconds. The plots, shown below in Figure 3, have a peak corresponding to the HBT effect. Note that the rates were normalized to the rates off the HBT peaks shown with red vertical lines in the right plot of Figure 2. These peaks were then fitted with a Gaussian to extract a t_0 and σ value of the distribution, which we use to calculate the oscillations in the pair rates in Section 4.3. To derive information on pair value oscillations, these calibrations were necessary as each peak occurs at a different t_0 due to minor path-length differences between each channel pair. Then the number of coincidences within the central peak region ($\pm 1.5\sigma$ window) was integrated over 20 second time bins for each channel pair, providing trending information for the coincidences over the full duration of the experiment.

As is apparent from Figure 3 in channel combinations on the same arm of the interferometer (1&2, 3&4), HBT peaks are suppressed in both the non-polarized and V-V polarized datasets. This is due to the Hong-Ou-Mandel (HOM) interference which competes with the HBT photon bunching. The HBT peaks in these combinations are not suppressed in the V-H polarized datasets, as the HOM effect only occurs between photons of the same polarization.
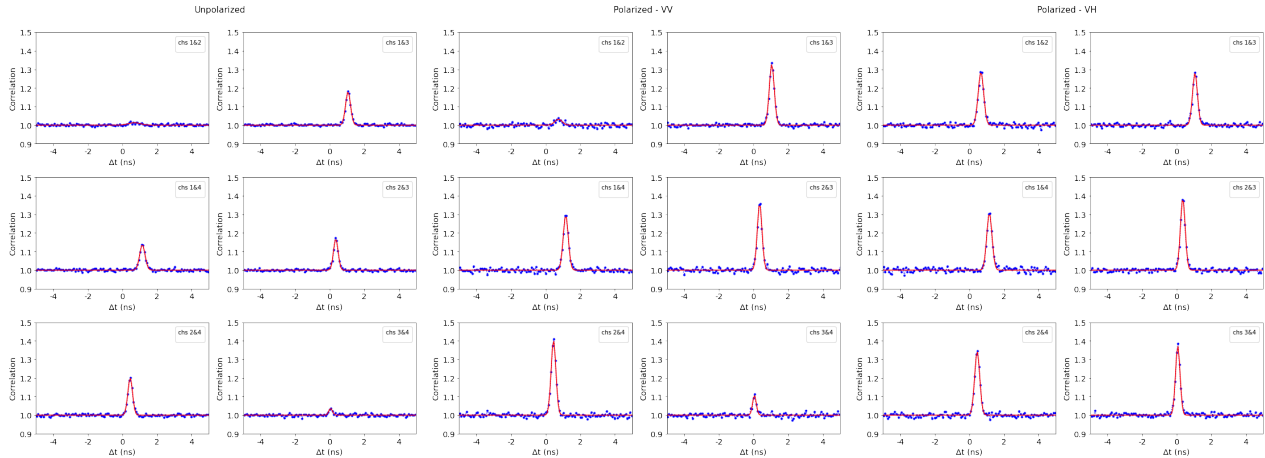
Figure 3. Normalized rates of two-photon detections as a function of relative time between them, for different output channel combinations and different input polarizations, as labeled. The peak in each case indicates the enhanced correlation between two photons from the same thermal source (HBT peaks), calibrating where simultaneous, indistinguishable pairs will appear. Left: Results with no polarizers at the interferometer input. Center: Results with aligned polarizers at the input. Right: Results with 90 degree cross polarizers at the input. See text for discussion.

4.3 Oscillation of coincidence rate

During data collection, one of the phase shifters was slowly advanced by the distance corresponding to a shift by several photon wavelengths. This was followed by a pause, then the second phase shifter repeated this process. As only one shifter was moving at a time, oscillations can be expected in the rates of photon pairs between outputs on opposite arms of the interferometer (e.g. Output 1 and Output 3) but not in outputs on the same arm (e.g. Output 1 and Output 2). Oscillations were present in the unpolarized datasets, with increased visibility in the polarized datasets with matching V-V polarization, see Figure 4. In the datasets where the polarizers were in 90 degrees cross polarized, V-H, these oscillations are not present.
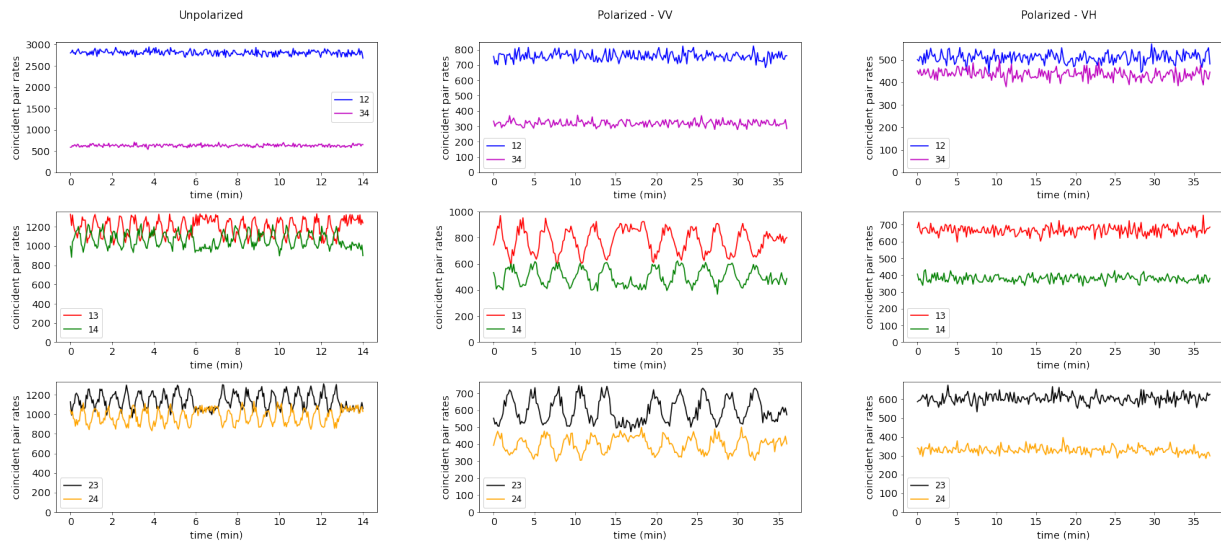
Figure 4. Rates of two-photon detections within a $\pm 1.5\sigma$ window about the t_0 of the HBT peak, fitted with a gaussian, versus time, where time corresponds to real time during which the phase shifters were moving a preset distance with a defined pause time in between each movement. Left: Results with no polarizers at the interferometer input, visibility is approximately 8%. Center: Results with aligned polarizers at the input, visibility is approximately 15%. Right: Results with 90 degree cross polarizers at the input. See text for discussion.

The movement of the phase shifters in the experiments simulate the effect that the Earth's rotation would have on incoming signals in the conceptual layout.[3, 20] This oscillatory behaviour as result of the phase shifting directly relates to the above Equation 1. We observe that combinations 1&3, 1&4 and 2&3, 2&4 oscillate in antiphase as expected.

5. CONCLUSION

In conclusion, we described a novel approach to astrometry employing two stars as sources of single mode photons, which interfere and produce specific patterns of coincidences. We presented results from the first experiments as important step in establishing the HBT effect and its variation as function of the phase difference in the context of timing performance of the single photon detectors. We also demonstrated in a bench-top setup that two-photon interference from quasi-thermal sources can be directly sensitive to their opening angle using path length variation for relative phase control. This principle can be extended to two-photon interference from two astronomical sources. With this demonstration, practical on-sky experiments are planned in the near future.

ACKNOWLEDGMENTS

REFERENCES

[1] ten Brummelaar, T. A., McAlister, H. A., Ridgway, S. T., W. G. Bagnuolo, J., Turner, N. H., Sturmann, L., Sturmann, J., Berger, D. H., Ogden, C. E., Cadman, R., et al., "First results from the CHARA array. II. a description of the instrument," *The Astrophysical Journal* **628**, 453–465 (July 2005).

[2] Pedretti, E., Monnier, J. D., ten Brummelaar, T., and Thureau, N. D., "Imaging with the CHARA interferometer," *New Astronomy Reviews* **53**, 353–362 (Nov. 2009).

[3] Stankus, P., Nomerotski, A., Složar, A., and Vintskevitch, S., "Two-photon amplitude interferometry for precision astrometry," *arXiv preprint arXiv:2010.09100* (2020).

[4] Nomerotski, A., Stankus, P., Složar, A., Vintskevich, S., Andrewski, S., Carini, G. A., Dolzhenko, D., England, D., Figueroa, E. V., Gera, S., Haupt, J., Herrmann, S., Katramatos, D., Keach, M., Parsells, A., Saira, O., Schiff, J., Svihra, P., Tsang, T., and Zhang, Y., "Quantum-assisted optical interferometers: instrument requirements," in [*Optical and Infrared Interferometry and Imaging VII*], Mérand, A., Sallum, S., and Tuthill, P. G., eds., *Proc. SPIE* (2020).

[5] Gottesman, D., Jennewein, T., and Croke, S., "Longer-baseline telescopes using quantum repeaters," *Phys. Rev. Lett.* **109**, 070503 (Aug 2012).

[6] Khabiboulline, E. T., Borregaard, J., De Greve, K., and Lukin, M. D., "Quantum-assisted telescope arrays," *Phys. Rev. A* **100**, 022316 (Aug 2019).

[7] Khabiboulline, E. T., Borregaard, J., De Greve, K., and Lukin, M. D., "Optical interferometry with quantum networks," *Phys. Rev. Lett.* **123**, 070504 (Aug 2019).

[8] Brown, M., Thiel, V., Allgaier, M., Raymer, M., Smith, B., Kwiat, P., and Monnier, J., "Interferometry-based astronomical imaging using nonlocal interference with single-photon states," in [*Frontiers in Optics + Laser Science 2021*], OSA (2021).

[9] Brown, M., Thiel, V., Allgaier, M., Raymer, M., Smith, B., Kwiat, P., and Monnier, J., "Long-baseline interferometry using single photon states as a non-local oscillator," in [*Quantum Computing, Communication, and Simulation II*], Hemmer, P. R. and Migdall, A. L., eds., SPIE (Mar. 2022).

[10] Brown, R. H. and Twiss, R. Q., "A test of a new type of stellar interferometer on sirius," *Nature* **178**, 1046–1048 (1956).

[11] Foellmi, C., "Intensity interferometry and the second-order correlation function $g^{(2)}$ in astrophysics," *Astronomy & Astrophysics* **507**, 1719–1727 (2009).

[12] Bojer, M., Huang, Z., Karl, S., Richter, S., Kok, P., and von Zanthier, J., "A quantitative comparison of amplitude versus intensity interferometry for astronomy," *New Journal of Physics* **24**(4), 043026 (2022).

[13] Gasparini, L., Bessire, B., Unternahrer, M., Stefanov, A., Boiko, D., Perenzoni, M., and Stoppa, D., "SUPERTWIN: towards 100kpixel CMOS quantum image sensors for quantum optics applications," in [*Quantum Sensing and Nano Electronics and Photonics XIV*], Razeghi, M., ed., *Proc. SPIE* (2017).

[14] Perenzoni, M., Pancheri, L., and Stoppa, D., "Compact spad-based pixel architectures for time-resolved image sensors," *Sensors* **16** (2016).

[15] Lee, M. and Charbon, E., "Progress in single-photon avalanche diode image sensors in standard CMOS: From two-dimensional monolithic to three-dimensional-stacked technology," *Japanese Journal of Applied Physics* **57**, 1002A3 (2018).

[16] Morimoto, K., Ardelean, A., Wu, M., Ulku, A. C., Antolovic, I. M., Bruschini, C., and Charbon, E., "Megapixel time-gated SPAD image sensor for 2d and 3d imaging applications," *Optica* **7**, 346 (2020).

[17] Divochiy, A., Marsili, F., Bitauld, D., Gaggero, A., Leoni, R., Mattioli, F., Korneev, A., Seleznev, V., Kaurova, N., Minaeva, O., Gol'tsman, G., Lagoudakis, K. G., Benkhaoul, M., Lévy, F., and Fiore, A., "Superconducting nanowire photon-number-resolving detector at telecommunication wavelengths," *Nature Photonics* **2**, 302–306 (2008).

[18] Zhu, D., Colangelo, M., Chen, C., Korzh, B. A., Wong, F. N. C., Shaw, M. D., and Berggren, K. K., "Resolving photon numbers using a superconducting nanowire with impedance-matching taper," *Nano Letters* (2020).

[19] Korzh, B., Zhao, Q., Allmaras, J. P., Frasca, S., Autry, T. M., Bersin, E. A., Beyer, A. D., Briggs, R. M., Bumble, B., Colangelo, M., Crouch, G. M., Dane, A. E., Gerrits, T., Lita, A. E., Marsili, F., Moody, G., Peña, C., Ramirez, E., Rezac, J. D., Sinclair, N., Stevens, M. J., Velasco, A. E., Verma, V. B., Wollman, E. E., Xie, S., Zhu, D., Hale, P. D., Spiropulu, M., Silverman, K. L., Mirin, R. P., Nam, S. W., Kozorezov, A. G., Shaw, M. D., and Berggren, K. K., "Demonstration of sub-3 ps temporal resolution with a superconducting nanowire single-photon detector," *Nature Photonics* **14**, 250–255 (2020).

[20] Chen, Z., Nomerotski, A., Složar, A., Stankus, P., and Vintskevitch, S., "Astrometry in two-photon interferometry using earth rotation fringe scan," *arXiv preprint arXiv:2205.09091* (2022).